

Nanopore sensors for nucleic acid analysis

Bala Murali Venkatesan^{1,2} and Rashid Bashir^{1,2,3*}

Nanopore analysis is an emerging technique that involves using a voltage to drive molecules through a nanoscale pore in a membrane between two electrolytes, and monitoring how the ionic current through the nanopore changes as single molecules pass through it. This approach allows charged polymers (including single-stranded DNA, double-stranded DNA and RNA) to be analysed with subnanometre resolution and without the need for labels or amplification. Recent advances suggest that nanopore-based sensors could be competitive with other third-generation DNA sequencing technologies, and may be able to rapidly and reliably sequence the human genome for under \$1,000. In this article we review the use of nanopore technology in DNA sequencing, genetics and medical diagnostics.

Sequencing the human genome has helped to improve our understanding of disease, inheritance and individuality. Genome sequencing has been critical in the identification of the genetic risk factors associated with complex human diseases^{1,2}, and continues to have an emerging role in therapeutics and personalized medicine. The growing need for cheaper and faster genome sequencing has prompted the development of new technologies that surpass conventional Sanger chain-termination methods in terms of speed and cost^{3,4}. These second- and third-generation sequencing technologies — inspired by the \$1,000 genome challenge proposed by the National Institutes of Health in 2004 (ref. 5) — are expected to revolutionize genomic medicine. Nanopore sensors are one of a number of DNA sequencing technologies that are currently poised to meet this challenge.

Nanopore-based sensing is attractive for DNA sequencing applications because it is a label-free, amplification-free, single-molecule approach that can be scaled for high-throughput DNA analysis. Moreover, it typically requires low reagent volumes, benefits from relatively low cost and supports long read lengths, so it could potentially enable *de novo* sequencing and long-range haplotype mapping. The principle of nanopore sensing is analogous to that of a Coulter counter⁶. A nanoscale aperture (the nanopore) is formed in an insulating membrane separating two chambers filled with conductive electrolyte. Charged molecules are driven through the pore under an applied electric potential (a process known as electrophoresis), thereby modulating the ionic current through the nanopore. This current reveals useful information about the structure and dynamic motion of the molecule.

The application of nanopores to DNA sequencing was first proposed by Church, Deamer, Branton, Baldarelli and Kasianowicz in a patent application that was filed in 1995 and awarded in 1998 (ref. 7). The basic idea is that when a single strand of DNA passes through the nanopore, the residual ionic current will depend on which nucleotide or base (adenine (A), cytosine (C), guanine (G) or thymine (T)) is in the nanopore at the time. Therefore, by recording how the ionic current through the nanopore changes with time, it should be possible to determine the sequence of bases in the DNA molecule. Using this general framework, proof-of-principle experiments using two naturally occurring, or biological, nanopores — α -haemolysin and *Mycobacterium smegmatis* porin A (MspA) — have shown that nanopore-based DNA sequencing is indeed feasible.

This Review focuses on recent progress in the field and will cover biological nanopores, solid-state nanopores (including graphene-based nanopores) and hybrids of the two. Nanopore-based medical

diagnostics and other non-sequencing applications will also be discussed. The major challenges in the field are to reduce the speed at which the DNA molecule passes, or translocates, through the nanopore (so that the bases can be reliably identified; Fig. 1) and to improve the sensitivity of the approach, which will require new sensing modalities and new device architectures (Table 1). More details on the history of nanopore-based DNA sensing can be found in previous reviews^{8–14}, and the challenges associated with nanopore sequencing are discussed in detail by Branton *et al.* in their review¹².

Biological nanopores

Biological nanopores inserted into lipid bilayers offer several advantages for single-molecule DNA analysis. First, cells can produce large numbers of biological nanopores with an atomic level of precision that cannot yet be replicated by the semiconductor industry; second, X-ray crystallography has provided information about the nanopore structure at ångström length scales; third, established genetic techniques (notably site-directed mutagenesis) can be used to tailor the physical and chemical properties of the nanopore; and fourth, remarkable heterogeneity is observed among biological nanopores in terms of size and composition.

In vitro studies of DNA transport through biological nanopores have traditionally involved the heptameric protein α -haemolysin. The channel through this protein nanopore comprises a 3.6-nm-diameter vestibule connected to a transmembrane β -barrel that is ~ 2.6 nm wide and ~ 5 nm long (Fig. 2a). However, the channel is just 1.4 nm wide at the point where the vestibule meets the β -barrel, which means that single-stranded DNA (ssDNA) can pass through the nanopore, but double-stranded DNA (dsDNA) cannot. Kasianowicz *et al.* first demonstrated the electrophoretic transport of individual ssDNA and ssRNA molecules through α -haemolysin¹⁵. In particular, early results demonstrated the ability of native α -haemolysin to distinguish between freely translocating RNA homopolymers of adenylic and cytidylic acid¹⁶, as well as polydeoxyadenylic acid and polydeoxycytidylic acid strands of ssDNA¹⁷, suggesting the potential emergence of α -haemolysin as a next-generation DNA sequencing tool.

However, developing a nanopore-based sequencing tool has been challenging, primarily because ssDNA moves through the nanopore at remarkably high velocities (estimated to be ~ 1 nucleotide per microsecond; Fig. 1) under typical experimental conditions. These velocities mean that only a small number of ions (as few as ~ 100) are available in the nanopore to correctly identify any given nucleotide, so the small changes in the ionic current due to

¹Department of Electrical and Computer Engineering, ²Micro and Nanotechnology Laboratory, ³Department of Bioengineering, University of Illinois at Urbana-Champaign, Urbana, Illinois 61820, USA. *e-mail: rbashir@illinois.edu

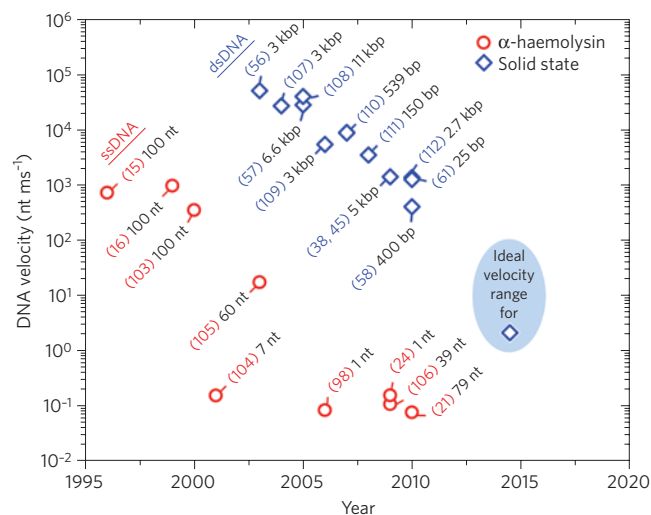


Figure 1 | Trends in nanopore analysis of DNA. DNA translocation velocity in nucleotides per millisecond (on a logarithmic scale) versus year for both ssDNA and dsDNA and for both α -haemolysin and solid-state nanopores. Each data point represents a reduction in translocation velocity or an improvement in sensitivity; for each data point the relevant reference(s) are shown in parentheses and the size of the shortest molecule detected is shown in nucleotides (nt), base pairs (bp) or kilobase pairs (kbp). For solid-state nanopore sequencing applications, the translocation velocity should be in the range 1–100 nt ms⁻¹ (pale blue region). Biological nanopores have already reached velocities below this range, and solid-state nanopores are also expected to approach these values around 2015. However, substantial improvements in sensitivity of both biological and solid-state nanopores are also needed, which is why researchers are exploring the new approaches described in Table 1. The reduced velocities (and improved sensitivities) for α -haemolysin have been achieved by a combination of site-specific mutagenesis and one of the following: the incorporation of DNA processing enzymes into the nanopore²¹, chemical labelling of the nucleotides¹⁰⁶ or the covalent attachment of an aminocyclodextrin adapter²⁴. The improvements in the performance of solid-state nanopores have been due to the optimization of solution conditions (temperature, viscosity, pH)¹⁰⁹, chemical functionalization¹¹⁰, surface-charge engineering⁴⁵, varying the thickness and composition of the membranes^{38,61,112}, and the use of smaller diameter nanopores^{58,61} (thereby enhancing polymer-pore interactions). This figure contains key nanopore developments in terms of translocation velocity and sensitivity, but is by no means exhaustive.

the presence of different nucleotides are likely to be overwhelmed by thermodynamic fluctuations (that is, statistical variations in the number of charge carriers and the position of the nucleotide in the pore). It has, therefore, proven impossible to sequence freely translocating ssDNA using α -haemolysin.

Most nanopore sequencing strategies so far have sought to actively or passively slow down the transport of ssDNA before readout. Active approaches typically incorporate enzymes to regulate DNA transport through the pore^{18–21}. An enzyme motor coupled to a nanopore is attractive for two reasons: (1) the enzyme–DNA complex forms in bulk solution, enabling it to be electrophoretically captured in the nanopore; (2) relatively slow and controlled motion is observed as the enzyme processively steps the DNA molecule through the nanopore. An elegant demonstration of this is the base-by-base ratcheting of ssDNA through α -haemolysin catalysed by DNA polymerase¹⁹. More recently, the processive replication of ssDNA on α -haemolysin using phi29 DNA polymerase was demonstrated²⁰. As well as being able to resolve individual catalytic cycles, polymerase dynamics (such as deoxyribonucleotide triphosphate (dNTP) binding and the opening and closing of polymerase fingers)

could also be discerned from measurements of the ionic current. Work on the controlled transport of DNA through α -haemolysin using enzymes was reviewed recently¹³.

Simpler, passive approaches to slowing down DNA also exist — such as nucleotide labelling, end termination of ssDNA with DNA hairpins and the use of positively charged residues in the nanopore as molecular ‘brakes’²² — but all require further work. Nucleotide labelling, for example, is attractive, as the possibility of varying the chemistry, charge and size of the label might enable direct, real-time sequencing²³, but it remains challenging to label contiguous nucleotides in large genomic fragments.

A more versatile, label-free sequencing method was recently demonstrated using resistive current measurements to continuously resolve indigenous mononucleotides (2′-deoxyadenosine 5′-monophosphate (dAMP), 2′-deoxycytidine 5′-monophosphate (dCMP), 2′-deoxyguanosine 5′-monophosphate (dGMP), and 2′-deoxythymidine 5′-monophosphate (dTMP))²⁴. Base selectivity was achieved by modifying a mutant α -haemolysin pore with an aminocyclodextrin adapter covalently attached within the β -barrel, thereby constricting the channel while enhancing the chemical specificity of the sensor. Raw mononucleotides were read with over 99% confidence under optimal operating conditions. By integrating this base identification platform with a highly processive exonuclease (through either chemical attachment or genetic fusion) to cleave and successively pass nucleotides to the nanopore, a single molecule ‘sequencing by digestion’ approach may indeed be feasible. Oxford Nanopore Technologies is currently developing a DNA sequencing technology based on this approach.

Although α -haemolysin has dominated the biological nanopore sequencing landscape so far, other more efficient biological nanopores are emerging. A structural drawback with α -haemolysin is that the cylindrical β -barrel can accommodate up to ~10 nucleotides at a time, all of which significantly modulate the pore current²⁵: this dilutes the ionic signature of the single nucleotide in the 1.4 nm constriction, thus reducing the overall signal-to-noise ratio in sequencing applications. The octameric protein channel MspA²⁶ does not suffer from this problem as it has a channel shaped like a tapered funnel that is just ~0.5 nm long, with a constriction of diameter ~1.2 nm at the point where it meets the vestibule (Fig. 2b).

Genetically engineered MspA can discriminate between trinucleotide sets (AAA, GGG, TTT, CCC) with an impressive 3.5-fold enhancement in nucleotide separation efficiency over native α -haemolysin²⁷. Moreover, in experiments involving immobilized ssDNA, as few as three nucleotides within or near the constriction contributed to the pore current²⁷ compared with the ten or so nucleotides that modulate the current in native α -haemolysin²⁵. By using additional genetic techniques (notably site-specific mutagenesis) it might be possible to achieve single-nucleotide resolution, but MspA-based sequencing also faces challenges. The speed of unimpeded ssDNA translocation through MspA is too fast to sequence ssDNA directly and in real time. Duplex interrupted nanopore sequencing²⁷ might be able to overcome this limitation by inserting a ‘short’ segment of dsDNA between each nucleotide in an analyte DNA molecule. As the converted DNA is driven through an MspA nanopore, each duplex temporarily halts the translocation process, allowing a single analyte nucleotide to be identified by measuring the ionic current. The duplex would then dissociate owing to the high electric field in the nanopore, allowing the DNA to advance to the next duplex and the next analyte nucleotide to be determined, and so forth. Such a method could ultimately enable fast and long sequential reads. However the ability to convert and read large genomic fragments with high fidelity using this approach has not yet been demonstrated.

Strand sequencing is an alternative to duplex interrupted sequencing that involves coupling an enzyme motor to a nanopore: this makes it possible to controllably step ssDNA through MspA,

Table 1 | Different sensing modalities for nanopore sensors and the challenges they face.

Sensing modality	Description of technique	Potential challenges	References
Ionic current	Hybridization-assisted nanopore sequencing	High spatial resolution required; complex algorithms needed for analysis.	97
	Sequencing by exonuclease digestion	Requires sequential passage of mononucleotides in the order in which they are cleaved.	24, 98
	Sequencing by synthesis	Retaining processing enzymes (DNA polymerase) at the pore; achieving long read lengths and maintaining enzyme activity under a voltage load.	18–21
	Duplex interrupted DNA sequencing	Converting large genomic ssDNA fragments to duplex interrupted structure.	27
Optical readout	Optical recognition of converted DNA	Complex and error-prone DNA conversion steps; high density, <2-nm-diameter nanopore arrays needed.	41
Transverse electron tunnelling	Tunnelling detector on a nanopore (metal, graphene, carbon nanotubes)	Precisely controlling orientation and position of nucleotides in the gap; slow translocation rates required to sufficiently sample over noise; nucleotide-dependent tunnelling currents need to be measured in solution.	84*, 86*, 93, 94, 99*
Capacitive sensing	Metal-oxide-semiconductor nanopore capacitor	Must operate in high-ionic-strength solution with negligible drift and leakage; DNA translocation rates need to be substantially reduced.	100, 101*, 102*

Nanopore sensors that operate by measuring ionic current have been successful in proof-of-principle sequencing experiments (notably those that rely on exonuclease digestion and duplex interruption). Sensors that employ optical readout show promise, but they require various DNA conversion steps (which are complex and error prone). Computational studies (marked with an asterisk) suggest that sensors that rely on electron tunnelling or capacitive sensing are capable of ultrafast sequencing, but this has not yet been demonstrated experimentally.

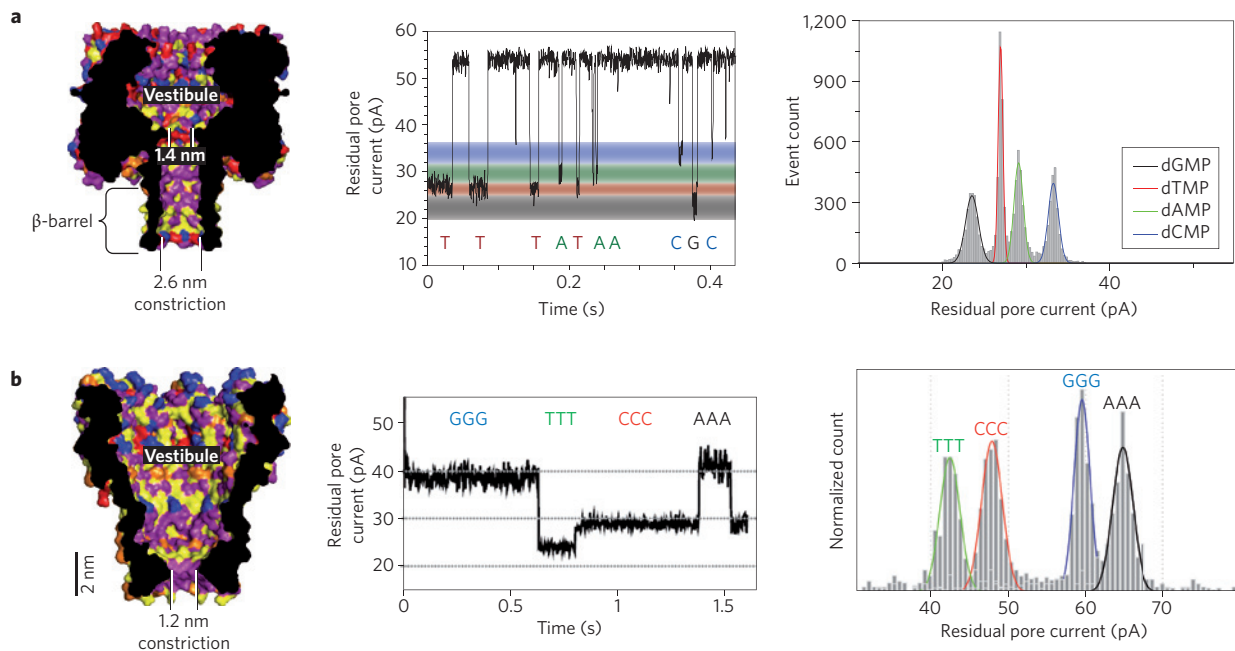


Figure 2 | Biological nanopores for DNA sequencing. a, Left: structural cross-section of α -haemolysin. The 1.4 nm constriction permits the passage of ssDNA but not dsDNA. Middle: typical plot of residual ionic current through an aminocyclodextrin-modified α -haemolysin nanopore versus time for individual mononucleotides (dAMP, dCMP, dGMP, dTMP). The reduction in the current caused by the passage of individual nucleotides through the nanopore is nucleotide dependent, facilitating identification. Right: histogram of the residual pore current based on measurements like those shown in the middle panel, which demonstrates how the different bases can be distinguished using ionic current alone under optimized conditions. **b**, Left: structural cross-section of MspA. Middle: typical plot of residual ionic current through an MspA nanopore versus time for a duplex interrupted DNA molecule (that contains a dsDNA segment (the duplex) between each ssDNA nucleotide triplet (AAA, TTT, GGG, CCC)). In this approach the duplex temporarily halts the passage of the DNA through the nanopore; when the duplex dissociates owing to the high electric field in the nanopore region, translocation starts again. A unique current level is observed for each triplet of nucleotides in a duplex interrupted molecule. Right: histogram showing that the separation efficiency of MspA is better than that of α -haemolysin. Figures reproduced with permission from: **a**, ref. 13, © 2010 Annual Reviews, Inc. (left panel) and ref. 24, © 2009 NPG (middle and right panels); **b**, ref. 27, © 2010 National Academy of Sciences.

with nucleotide identification occurring at each step. Candidate enzymes suited for this application include T7 DNA polymerase, Klenow fragment of DNA polymerase 1 and phi29 DNA polymerase^{18,20,21}. The last of these is known to be remarkably stable and highly efficient at catalysing sequential nucleotide additions in α -haemolysin²⁰. It is plausible, therefore, that long strands of DNA could be sequenced by coupling phi29 DNA polymerase to MspA, although this has not yet been demonstrated experimentally.

Biological nanopores also have tremendous potential for applications other than DNA sequencing. The connector protein from the bacteriophage phi29 DNA packaging motor, for example, could prove useful for applications in molecular diagnostics and DNA fingerprinting. The channel in this protein nanopore is approximately 3.6 nm wide, and it opens into a vestibule with inner diameter of ~6 nm. Moreover, it has an open channel conductance that is approximately five times higher than that of α -haemolysin under similar conditions. This suggests the possibility of screening larger analytes such as dsDNA, DNA protein complexes and amino acid polymers for protein sequencing. The translocation of dsDNA through a genetically engineered connector channel embedded in a lipid bilayer was recently demonstrated²⁸. Unidirectional transport of dsDNA through this channel (from amino-terminal entrance to carboxyl-terminal exit) was also observed²⁹, suggesting a natural valve mechanism in the channel that assists dsDNA packaging during bacteriophage phi29 virus maturation. The capabilities of this protein nanopore will become more apparent in years to come.

Despite the heterogeneity and remarkable sensitivity of biological nanopores, they also have some inherent disadvantages: the mechanical instability of the lipid bilayer that supports the nanopore; the sensitivity of biological nanopores to experimental conditions (such as pH, temperature and salt concentration); and the difficulty in integrating biological systems into large-scale arrays. The stability of the

bilayer can be improved by supporting it on solid and nanoporous substrates^{30–33}, by varying its compositions^{34,35} or by using tethered bilayer architectures³⁶. However, as we shall see in the next section, solid-state nanopores are considerably more robust and durable.

Solid-state nanopores

Solid-state nanopores are fast becoming an inexpensive and highly versatile alternative to biological nanopores. As well as robustness and durability, the solid-state approach offers the ability to tune the size and shape of the nanopore with subnanometre precision^{37,38}, the ability to fabricate high-density arrays of nanopores³⁹, superior mechanical, chemical and thermal characteristics compared with lipid-based systems, and the possibility of integrating with electronic⁴⁰ or optical readout techniques⁴¹.

The first reports of DNA sensing using solid-state nanopores emerged in early 2001 when Golovchenko and co-workers used a custom-built ion-beam sculpting tool with feedback control to make nanopores with well-defined sizes in thin SiN membranes⁴². Now, most groups prefer to use a focused electron beam with a probe that is a few nanometres in diameter to sputter nanopores in thin insulating membranes, a technique that has evolved since the 1980s⁴³. The fabrication of solid-state nanopores in thin insulating membranes has been reviewed elsewhere⁴⁴, as have applications to single-molecule biophysics¹⁰. SiN has traditionally been the nanopore membrane material of choice owing to its high chemical resistance and low mechanical stress. These membranes have traditionally been fabricated by an optimized low-pressure chemical vapour deposition process, typically at elevated temperatures (~800 °C), but this process does not offer the subnanometre control over membrane thickness that is needed to probe DNA with single-nucleotide resolution.

In working towards developing ultrathin membranes, one of us (R.B.) and co-workers have shown that atomic-layer deposition

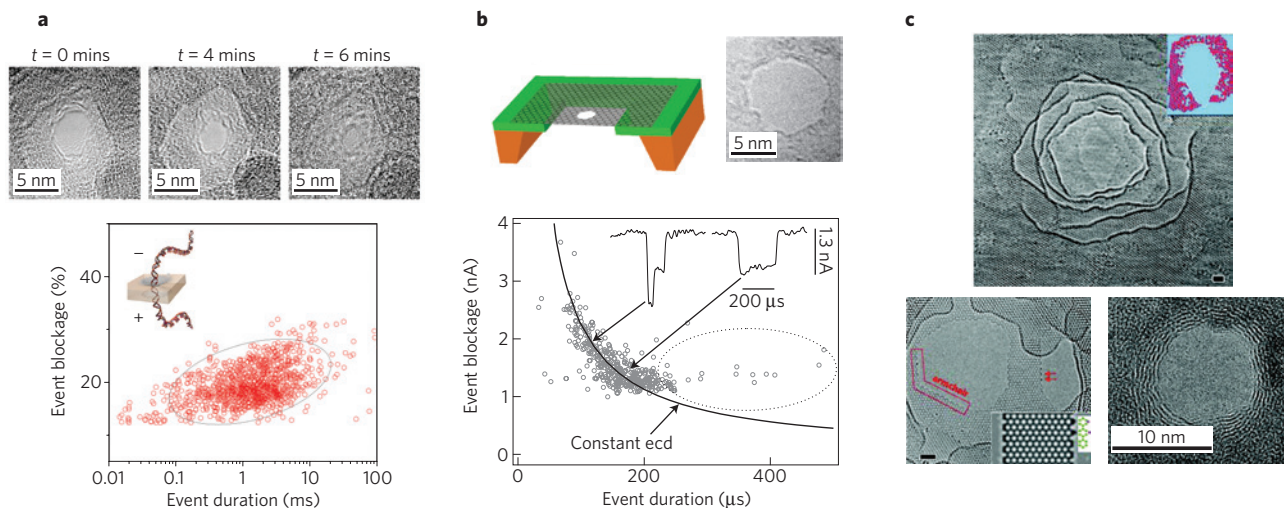


Figure 3 | Solid-state nanopore architectures for DNA analysis. **a**, Top: TEM images showing the formation (by a focused electron beam) and controlled contraction of nanopores in Al_2O_3 membranes. It is possible to control the diameter of the nanopore with subnanometre precision. Bottom: scatter plot of event blockage (the percentage of open pore ionic current that is blocked as a molecule passes through the pore) versus event duration (on a logarithmic scale) for the translocation of segments of dsDNA containing 5,000 base pairs through a 5-nm-diameter Al_2O_3 pore showing a single blockage level (~20% of the open pore current) corresponding to linear, unfolded dsDNA transport. **b**, Top: schematic (left) and TEM image (right) of a nanopore in a suspended graphene film containing just one to two layers of carbon atoms. Bottom: scatter plot of event blockage versus event duration showing that folded DNA (left of inset, deep blockade level) and unfolded DNA (right of inset, shallow blockade level) can be distinguished. The solid line represents a constant event charge deficit (ecd) which is the total area under each current transient resulting from a DNA translocation event). As shown, fast high-amplitude events and slow low-amplitude events can share a constant ecd or constant area, signifying folded and unfolded translocation events respectively. **c**, Top: TEM image of a terraced nanopore formed in a graphene film containing ~10 monolayers of carbon atoms. Scale bar, 1 nm. Bottom left: nanopore in a monolayer of graphene with primarily armchair edges surrounded by multilayered regions. Scale bar, 1 nm. Bottom right: TEM image of a nanopore in multilayer graphene; ripples at the pore edge again show the terraced structure. Figures reproduced with permission from: **a**, ref. 38, © 2009 Wiley and ref. 45, © 2010 Wiley (inset); **b**, ref. 51, © 2010 NPG; **c**, ref. 55, © 2011 ACS (top and bottom left panels) and ref. 52, © 2010 ACS (bottom right panel).

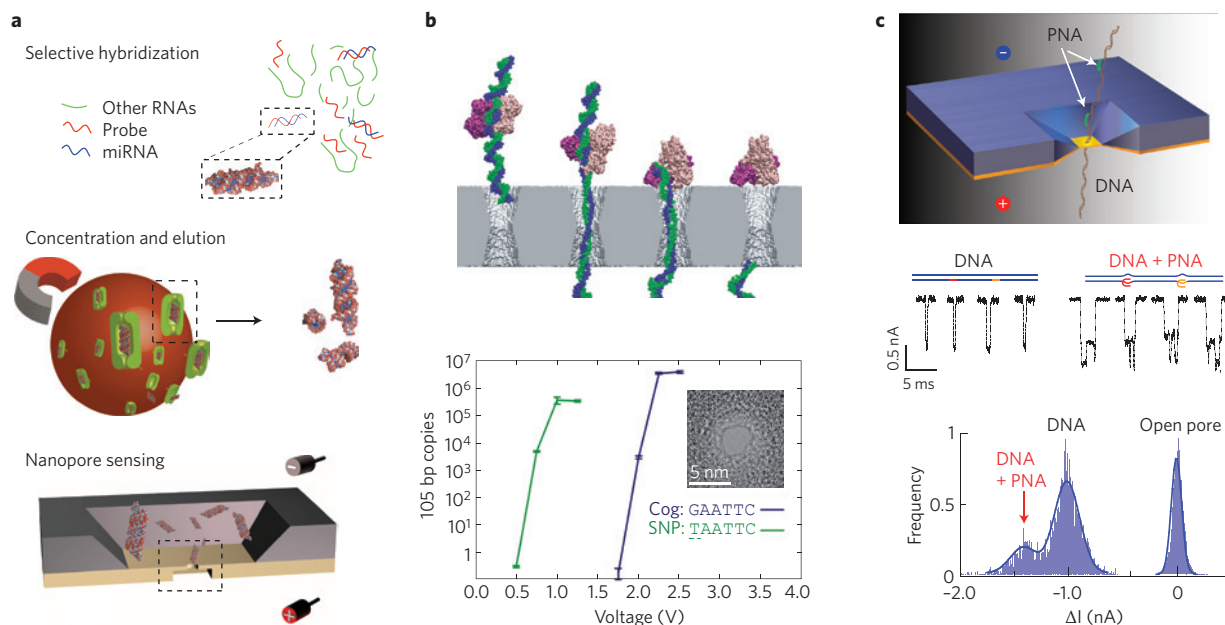


Figure 4 | Other applications of nanopores: miRNA detection and genomic profiling. **a**, Probe-specific hybridization is used to separate and concentrate sequence-specific miRNAs from tissue samples; nanopore-based sensors are then used to measure the level of miRNAs. This technique offers comparable sensitivity to conventional microarray techniques. **b**, Sequences containing single nucleotide polymorphisms (SNPs) have been detected with nanopore-based techniques. Top: protein-bound dsDNA complexes (105 base pairs (bp) long) were electrophoretically driven into a ~2-nm-diameter nanopore and then sheared. Bottom: the shearing occurs when the voltage across the nanopore exceeds a threshold (purple line), thereby dislodging the protein and allowing the electrophoretic transport of the 105 bp fragment through the nanopore. Cog refers to the cognate protein binding sequence. Note: the y axis here represents the number of copies of 105 bp DNA that have translocated through the nanopore as a result of protein shearing (and measured by quantitative PCR). Changing just one nucleotide in the protein binding sequence caused the threshold voltage to drop (green line), thus allowing SNPs to be detected. The inset shows a TEM image of the nanopore. **c**, Genomic profiling. Top: Schematic showing translocation of PNA-tagged DNA molecules through a solid-state nanopore. Middle: PNA-tagged dsDNA complexes produced unique current transients in nanopore measurements. Bottom: the number of PNA tags per molecule can be quantified, facilitating rapid electrical profiling of DNA molecules. Figures reproduced with permission from: **a**, ref. 61, © 2010 NPG; **b**, ref. 68, © 2007 ACS; **c**, ref. 69, © 2010 ACS.

(ALD) can be used to make Al₂O₃ membranes, with ångström-level control over membrane thickness³⁸, and that two interesting phenomena occur when a focused electron beam is used to sputter nanopores in these metal oxide membranes. First, the Al₂O₃, which is an insulator, is partially converted into metallic Al, in a dose-dependent way — this process could potentially be used to ‘write’ nanoscale electrodes in the pore. Second, different nanocrystalline domains are formed in a dose-dependent manner, which could potentially allow patterning of the surface charge at the interface between the nanopore and the electrolyte⁴⁵. Controlling the stoichiometry of the material in the nanopore and/or the surface charge density could allow researchers to reduce 1/f noise⁴⁶ and DNA translocation velocities. Indeed, we observed that DNA translocation was slower in Al₂O₃ nanopores than in SiN nanopores with similar diameters, which was attributed to the strong electrostatic interactions between the positively charged Al₂O₃ surface and the negatively charged dsDNA⁴⁵. Enhancing these interactions, either electrostatically or chemically, could reduce DNA velocities even more. The ALD approach should also allow nanopores to be formed in a variety of other high-dielectric-constant materials, including TiO₂ and HfO₂, each of which has unique material properties. Moreover, ALD is a relatively low-temperature (typically <250 °C) process⁴⁷ so it should be possible to integrate metallic contacts and graphene layers directly into the membrane. Though the ALD approach to membrane fabrication has shown promise, the fabrication of robust, insulating, subnanometre-thick membranes has been challenging owing to ionic current leakage through pinholes in ultrathin membranes.

Graphene, a two-dimensional sheet of carbon atoms, may be the answer to these problems because it possesses remarkable

mechanical, electrical and thermal properties⁴⁸. Moreover, the thickness of a single layer of graphene is comparable to the spacing between nucleotides in ssDNA (0.32–0.52 nm), which makes it particularly attractive for electronic DNA sequencing. In 2008 Drndic and co-workers were the first to fabricate single nanopores and nanopore arrays in suspended graphene films⁴⁹, and subsequent *in situ* transmission electron microscopy (TEM)-based studies elucidated the kinetics of pore formation and edge stability in graphene⁵⁰. Subsequently groups led by Golovchenko⁵¹, Drndic⁵² and Dekker⁵³ detected individual dsDNA molecules using nanopores in suspended graphene films: the films had been prepared either by chemical vapour deposition or exfoliation from graphite, and the nanopores (which had diameters in the range 2–25 nm) were produced by a focused electron beam. Nanopores were formed in membranes containing as few as one to two layers of carbon atoms, all of which exhibited remarkable durability and insulating properties in high-ionic-strength solution, although there were some intriguing differences in the results.

Golovchenko and co-workers⁵¹ found that the conductance of the nanopore was proportional to the pore diameter for membranes containing just one layer of graphene, whereas the conductance is typically proportional to the square of the diameter for SiN membranes, which are much thicker³⁹. An effective membrane thickness, $h_{\text{eff}} \sim 0.6$ nm, was extracted for monolayer graphene membranes⁵¹, which agrees with theory in the limit $h_{\text{eff}} \rightarrow 0$, where the dominant resistance is the access resistance R_{access} , which is inversely proportional to the pore diameter⁵⁴, rather than the pore resistance R_{pore} . (R_{access} is attributed to the potential drop in the electrolyte from the electrode to the nanopore.)

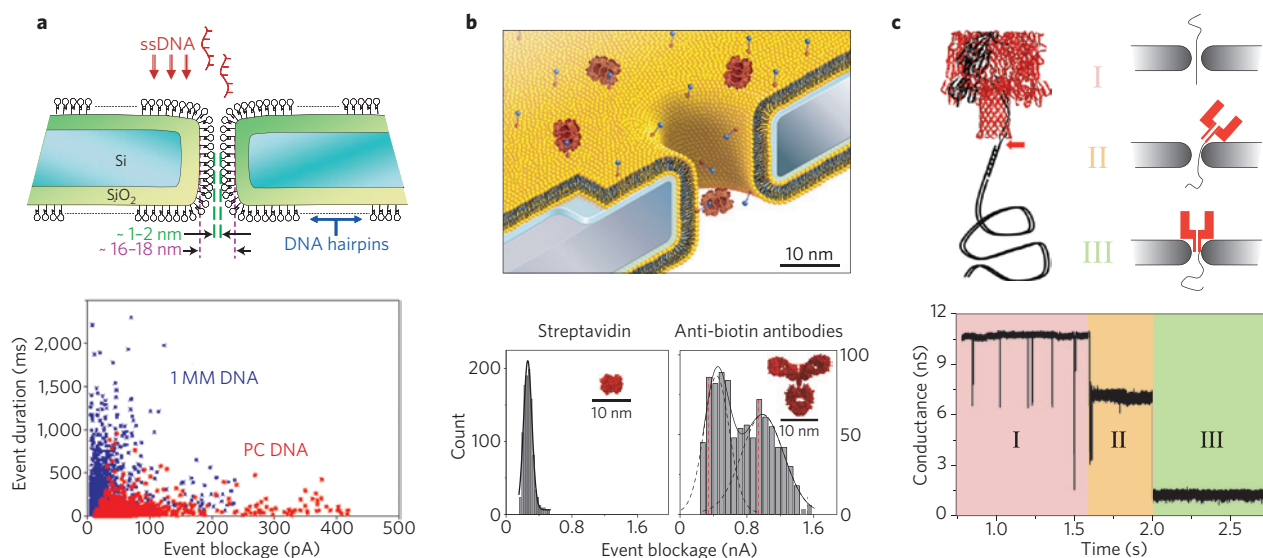


Figure 5 | Hybrid biological-solid-state nanopores. **a**, A SiO₂ nanopore functionalized with hairpin DNA (top) can distinguish between ssDNA that is perfectly complementary (PC DNA) to the hairpin sequence (bottom, red data points) and ssDNA that differs by a single base (bottom, blue data points; 1MM, one base mismatch), thereby allowing for the detection of SNPs. **b**, A SiN nanopore coated with a fluid lipid bilayer containing mobile ligands attached to the surface (top) can detect and differentiate various protein analytes because they lead to different current blockage distributions as shown in the histograms (bottom). **c**, α -haemolysin can be inserted into a SiN nanopore by attaching a dsDNA tail that can be pulled through the nanopore by electrophoresis (top left). The formation of the hybrid nanopore occurs in three stages (top right), each of which is associated with a characteristic conductance (bottom). When the α -haemolysin has been inserted into the SiN nanopore (stage III), the conductance is consistent with values measured for α -haemolysin in a lipid bilayer. Figures reproduced from: **a**, ref. 70, © 2007 NPG; **b**, ref. 74, © 2011 NPG; **c**, ref. 75, © 2010 NPG.

However, Dekker and co-workers⁵³ found that the pore conductance was proportional to the square of the diameter, which suggests that the thickness of the membrane was not negligible (that is, $R_{\text{pore}} > R_{\text{access}}$). The origin of this behaviour might be the polymer coating (16-mercaptohexadecanoic acid) that was used to coat the graphene to reduce DNA adsorption. They also found that the conductance for a given diameter of nanopore remained largely constant as the number of graphene layers in the membrane was increased from one to eight⁵³. This result is plausible as nanopore formation in multilayer graphene is known to induce a terrace effect, with the number of layers increasing as we move away from the pore (Fig. 3c). This effect was confirmed recently using TEM image analysis⁵⁵, and is also visible in earlier studies⁴⁹. A terraced nanopore architecture could prove very useful for two reasons: (1) it potentially relaxes the constraint of growing and transferring a large-area monolayer to fabricate a graphene monolayer nanopore; and (2) a multilayered support may increase the stability and longevity of a graphene nanopore sensor.

The translocation of dsDNA through graphene nanopores induced subtle fluctuations in the ionic current, indicating the translocation of both folded and unfolded DNA structures^{51–53}, analogous to the DNA-induced current blockades seen in SiN nanopores^{56,57}. Translocation velocities were between about 10 and 100 nucleotides per microsecond, which is too fast for the electronic measurement of individual nucleotides. However, computer simulations of dsDNA passing through a 2.4-nm-diameter nanopore in a ~0.6-nm-thick graphene membrane revealed a resolution of ~0.35 nm, which is similar to the size of an individual DNA nucleotide⁵¹. This result suggests that if the translocation speed could be reduced to roughly one nucleotide per millisecond, single-nucleotide detection should be possible, which could potentially lead to DNA sequencing with electronic readout.

To enable such advancements, however, we need a better understanding of the quantitative aspects of DNA translocation. Why, for example, do nanopores in multilayer graphene (3–15 monolayers)⁵² give deeper DNA-induced current blockades than nanopores in

single-layer graphene under normalized conditions⁵¹. One possible explanation is the terrace effect described above, but the structure of graphene nanopores needs to be studied in greater detail.

There are also various fundamental questions about sequencing with graphene nanopores that remain unanswered. For example, is single-nucleotide resolution possible in the presence of thermodynamic fluctuations and electrical noise? And will the chemical and structural similarity of the purines (A and G) and the pyrimidines (C and T) inherently limit the identification of individual nucleotides using ionic current? Surface functionalization might enhance the nucleotide specificity of graphene nanopores, but it could also compromise resolution by increasing the thickness of the membrane. Without doubt, this exciting yet preliminary work will certainly be the precursor for many future studies of graphene nanopores.

Other applications of nanopores

The more immediate application for solid-state nanopores is likely to be in medical diagnostics. A nanopore-based diagnostic tool could offer various advantages: it could detect target molecules at very low concentrations from very small sample volumes⁵⁸; it could simultaneously screen panels of biomarkers or genes (which is important in disease diagnosis, monitoring progression and prognosis); it could provide rapid analysis at relatively low cost; and it could eliminate cumbersome amplification and conversion steps such as PCR, bisulphite conversion and Sanger sequencing.

MicroRNA (miRNA) expression profiling is one application where solid-state nanopore technology could excel. The detection and accurate quantification of these cancer biomarkers will have important clinical implications, facilitating disease diagnosis, staging, progression, prognosis and treatment response^{59,60}. It was recently demonstrated that a nanopore-based approach for the detection of specific microRNA sequences enriched from cellular tissue can achieve sensitivities that are comparable to conventional microarray technologies (Fig. 4a)⁶¹.

Another potential application for solid-state nanopores is epigenetic analysis — more specifically the detection of aberrant DNA methylation, which can serve as a robust biomarker in cancer⁶² (for example, GSTP1 promoter hypermethylation is observed in over 90% of prostate cancer cases)⁶³. Aberrant methylation can also be an indicator of disease severity and metastatic potential in many tumour types^{62,64}. Preliminary progress towards nanopore-based methylation analysis has been reported, including the detection of methylated⁶⁵ and hydroxymethylated DNA⁶⁶, but this application is still in its infancy.

Genetic analysis involving the detection of single nucleotide polymorphisms (SNPs) is another important diagnostic application for which nanopores may be well suited. SNPs and point mutations have been linked to a variety of mendelian diseases as well as more complex disease phenotypes⁶⁷. In proof-of-principle experiments, SNPs have been detected using ~2-nm-diameter SiN nanopores⁶⁸. Using the nanopore as a local force actuator, the binding energies of a DNA binding protein and its cognate sequence relative to a SNP sequence could be discriminated (Fig. 4b). This approach could be extended to screen mutations in the cognate sequences of various other DNA binding proteins, including transcription factors, nucleases and histones.

The genomic profiling of viruses and human pathogens using solid-state nanopores is also attractive. An innovative approach involving the introduction of highly invasive peptide nucleic acid (PNA) probes has been used to label target genomes with high affinity and sequence specificity, creating local bulges (P loops) in the molecule⁶⁹. Translocation of this labelled molecule resulted in secondary DNA–PNA blockade levels (Fig. 4c), effectively ‘barcoding’ a target genome. Although further studies are needed to determine the ultimate spatial resolution of this technique, it could potentially enable the rapid, accurate and amplification-free identification of small (5–10 kilobase) viral genomes including hepatitis C, dengue fever and West Nile virus.

Hybrid biological–solid-state nanopores

A major drawback with solid-state nanopore technology at present is that it cannot chemically differentiate between analytes of approximately the same size. This lack of chemical specificity can be overcome by attaching specific recognition sequences and receptors to the nanopore to create a hybrid structure^{70,71} that has the potential to uniquely identify nucleotides in sequencing applications, or to differentiate and quantify target proteins in diagnostic applications. Chemical functionalization and its effect on the electrical properties of polymer nanopores was recently reviewed⁷².

Surface functionalization can also be used to introduce DNA sequence specificity. In studies involving SiO₂ nanopores functionalized with hairpin DNAs, higher fluxes and shorter translocation times were observed for the passage of perfectly complementary ssDNA compared with ssDNA in which there was a single base mismatch, demonstrating the potential of this approach to detect SNPs (Fig. 5a)⁷⁰. Functionalized biomimetic nanopores in SiN have furthermore enabled the study of nucleocytoplasmic transport phenomena at the single-molecule level⁷³.

Altering the surface chemistry of a nanopore can also facilitate the sensitive detection and discrimination of proteins. Drawing inspiration from the lipid-coated olfactory sensilla of insect antennae, SiN nanopores coated with a fluid lipid bilayer were recently used to identify proteins (Fig. 5b)⁷⁴. The incorporation of mobile ligands into the bilayer introduced chemical specificity into the nanopore, slowed the translocation of target proteins, prevented pores from clogging and eliminated non-specific binding, thereby resolving many issues inherent to solid-state nanopores. A lipid-bilayer-coated nanopore architecture of this nature (in either SiN (ref. 74) or Al₂O₃ (ref. 33)) could also, in principle, be integrated with biological nanopores to form robust nanopore sequencing elements.

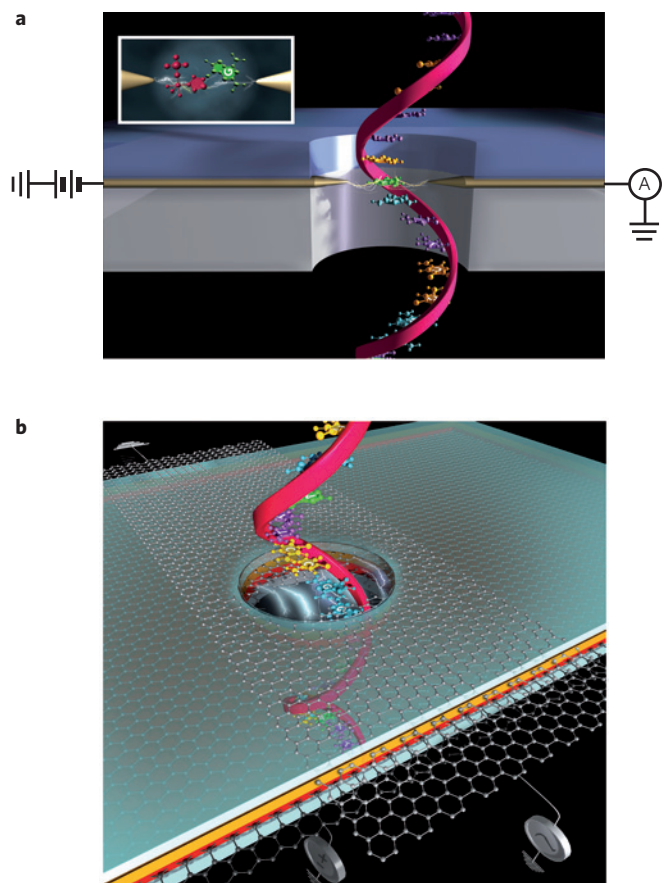


Figure 6 | Possible novel nanopore architectures for sequencing.

a, Schematic cross-section showing ssDNA passing through a solid-state nanopore with an embedded tunnelling detector⁹². The detector consists of two electrodes spaced ~1 nm apart on opposite sides of the nanopore. Changes in the tunnelling current as ssDNA passes through the nanopore (and between the electrodes) could be used to identify the sequence of bases in the DNA. Inset: top view showing a nucleotide positioned in the nanogap between the electrodes of the tunnelling detector. Figure reproduced from ref. 92, © 2010 NPG. **b**, Schematic showing ssDNA passing through a solid-state nanopore with an embedded graphene gate and a graphene nanoribbon on the membrane containing the nanopore; both the gate and the nanoribbon contain circular openings for the DNA to pass through. The graphene gate could be used to induce either p-type or n-type behaviour in the nanoribbon and to electrostatically slow down ssDNA. Changes in the transverse conductance of the nanoribbon as ssDNA passes through the nanopore could be used to identify the sequence of bases in the DNA⁸⁴. Functionalization of the edges of the circular opening in the nanoribbon could further enhance nucleotide-specific interactions.

The concept of hybrid biological–solid-state nanopores took another step forward recently when a genetically engineered α -haemolysin protein channel was inserted into nanopore in a SiN membrane (Fig. 5c)⁷⁵. By chemically linking a long dsDNA tail to α -haemolysin, it could be electrophoretically guided into the SiN nanopore to form a coaxially aligned structure. Measurements of nanopore conductance and ssDNA translocation times were in good agreement with α -haemolysin embedded in lipid bilayers⁷⁶, but blockade amplitudes were significantly less, which was attributed to deformation of the biological nanopore and leakage currents, and an increase in electrical noise was also observed. These parameters will probably need to be optimized to match

the single nucleotide sensitivity of aminocyclodextrin-modified α -haemolysin²⁴. Nevertheless, this hybrid architecture opens up the exciting possibility of combining the single-nucleotide recognition capabilities of α -haemolysin or MspA with wafer-scale arrays of individually addressed solid-state nanopores for high-throughput sequencing applications.

Outlook

The advances described here suggest that nanopores are likely to have an increasing role in medical diagnostics and DNA sequencing in years to come, but they will face competition from a number of other techniques. These include single-molecule evanescent field detection of sequencing-by-synthesis in arrays of nanochambers (Pacific Biosciences)⁷⁷, sequencing by ligation on self-assembled DNA nanoarrays (Complete Genomics)⁷⁸, and the detection of H⁺ ions released during sequencing-by-synthesis on silicon field-effect transistors from multiple polymerase-template reactions (Ion Torrent)⁷⁹. However, the possibility of using nanopore-based sensors to perform long base reads on unlabelled ssDNA molecules in a rapid and cost-effective manner could revolutionize genomics and personalized medicine, which is why public bodies such as the National Institutes of Health⁸⁰ in the US and private-sector companies such as IBM, Oxford Nanopore Technologies and NABsys, are continuing to invest heavily in nanopore-based DNA sequencing technology.

Current trends suggest that many challenges in sequencing with biological nanopores (the high translocation velocity and the lack of nucleotide specificity) have been resolved. Similarly, given the progress with solid-state nanopores, if the translocation velocity could be reduced to a single nucleotide (which is $\sim 3\text{\AA}$ long) per millisecond, and if nucleotides could be identified uniquely with an electronic signature (an area of intense research), it would be possible to sequence a molecule containing one million bases in less than 20 minutes. Furthermore, if this technology could be scaled to an array of 100,000 individually addressed nanopores operating in parallel, it would be possible to sequence an entire human genome (some three billion base pairs) with 50-fold coverage in less than one hour.

Achieving this goal will require novel device architectures that complement or replace ionic current readout with more sophisticated readout methods. There have been preliminary reports on the use of embedded planar gate electrodes in nanopores⁴⁰ and nanochannels^{81,82} to electrically modulate the ionic pore current, and the integration of single-walled carbon nanotubes for the translocation of ssDNA⁸³. Theorists, meanwhile, have proposed embedding graphene nanoribbons^{84,85} and nanogaps^{86,87} in nanopores to enable electronic readout of individual nucleotides, but issues such as the electrochemistry at the graphene/fluid interface, the reproducibility of the electronic properties of the graphene edges and the chemical functionalization of these edges need to be addressed. An alternative architecture, termed the DNA nanopore transistor, has been proposed by IBM researchers. Using molecular dynamics, the IBM team recently demonstrated the controlled base-by-base ratcheting of ssDNA through a nanopore in a multilayer metal oxide membrane (driven by alternating electric fields applied across the metal layers)⁸⁸, but this result has yet to be confirmed in experiments.

Recent experiments with scanning tunnelling microscopes suggest that it might be possible to identify nucleotides with electron tunnelling⁸⁹ (because the energy gaps between the highest occupied and lowest unoccupied molecular orbitals of A, C, G and T are unique⁹⁰), and partially sequence DNA oligomers⁹¹. Nanofabricated metallic gap junctions have also been used to identify single nucleotides by measuring electron tunnelling currents⁹². Neither of these experiments involved nanopores, but if a tunnelling detector of this nature could be embedded in a solid-state nanopore, and the DNA translocation velocity could be reduced, it may become possible to directly sequence DNA with a solid-state nanopore (Fig. 6).

Efforts to fabricate nanopore sensors that contain nanogap-based tunnelling detectors are currently underway^{93,94}, but thermal fluctuations and electrical noise present major challenges. One solution could be to adopt a statistical approach that involves repeatedly sampling each nucleotide or molecule to determine the sequence of bases. Another challenge is the fact that tunnelling currents vary exponentially with both the width and the height of the barriers that electrons have to tunnel through, which in turn depends on the effective tunnel distance and on molecule orientation. A four-point-probe measurement could therefore reveal significantly more information than the two-probe measurements attempted so far, but reliably fabricating such a four-probe structure with subnanometre precision will be a formidable challenge. It should also be noted that it is not necessary to uniquely identify all four bases for certain applications. Some researchers have used a binary conversion of nucleotide sequences (A or T = 0, and G or C = 1), to discover biomarkers and identify genomic alterations in short fragments of DNA and RNA^{95,96}.

Over the past few years both biological and solid-state nanopores have been moving closer to the goal of direct label-free sequencing of DNA molecules in real time. There is no doubt that nanopore-based sensors will continue to develop as strong candidates to join other third-generation sequencing technologies in the race towards affordable and personalized DNA sequencing.

References

1. Thomas, P. D. & Kejariwal, A. Coding single-nucleotide polymorphisms associated with complex vs. mendelian disease: Evolutionary evidence for differences in molecular effects. *Proc. Natl Acad. Sci. USA* **101**, 15398–15403 (2004).
2. International HapMap Consortium. A haplotype map of the human genome. *Nature* **437**, 1299–1320 (2005).
3. Mardis, E. R. Next-generation DNA sequencing methods. *Annu. Rev. Genom. Hum. Genet.* **9**, 387–402 (2008).
4. Metzker, M. L. Sequencing technologies — the next generation. *Nature Rev. Genet.* **11**, 31–46 (2010).
5. <http://www.genome.gov/12513210>.
6. Coulter, W. H. Means for counting particles suspended in a fluid. US patent 2,656,508 (1953).
7. Church, G., Deamer, D. W., Branton, D., Baldarelli, R. & Kasianowicz, J. Characterization of individual polymer molecules based on monomer-interface interactions. US patent 5,795,782 (1995).
8. Deamer, D. W. & Branton, D. Characterization of nucleic acids by nanopore analysis. *Acc. Chem. Res.* **35**, 817–825 (2002).
9. Rhee, M. & Burns, M. A. Nanopore sequencing technology: research trends and applications. *Trends Biotechnol.* **24**, 580–586 (2006).
10. Dekker, C. Solid-state nanopores. *Nature Nanotech.* **2**, 209–215 (2007).
11. Healy, K. Nanopore-based single-molecule DNA analysis. *Nanomedicine* **2**, 459–481 (2007).
12. Branton, D. *et al.* The potential and challenges of nanopore sequencing. *Nature Biotechnol.* **26**, 1146–1153 (2008).
This review article assesses the feasibility of various nanopore sequencing techniques that are currently under development (both optical and electrical).
13. Deamer, D. W. Nanopore analysis of nucleic acids bound to exonucleases and polymerases. *Annu. Rev. Biophys.* **39**, 79–90 (2010).
This review article provides a historical perspective on the field of nanopore DNA sequencing and elaborates on nanopore-based enzyme-mediated sequencing approaches.
14. Iqbal, S. & Bashir, R. *Nanopores: Sensing and Fundamental Biological Interactions* (Springer, 2011).
15. Kasianowicz, J. J., Brandin, E., Branton, D. & Deamer, D. W. Characterization of individual polynucleotide molecules using a membrane channel. *Proc. Natl Acad. Sci. USA* **93**, 13770–13773 (1996).
This is the first experimental report of electronic detection of a DNA molecule passing through a nanopore (α -haemolysin) and marks the start of the nanopore sequencing field.
16. Akeson, M., Branton, D., Kasianowicz, J. J., Brandin, E. & Deamer, D. W. Microsecond time-scale discrimination among polycytidylic acid, polyadenylic acid, and polyuridylic acid as homopolymers or as segments within single RNA molecules. *Biophys. J.* **77**, 3227–3233 (1999).
17. Meller, A. & Branton, D. Single molecule measurements of DNA transport through a nanopore. *Electrophoresis* **23**, 2583–2591 (2002).

18. Benner, S. *et al.* Sequence-specific detection of individual DNA polymerase complexes in real time using a nanopore. *Nature Nanotech.* **2**, 718–724 (2007).
19. Cockroft, S. L., Chu, J., Amarin, M. & Ghadiri, M. R. A single-molecule nanopore device detects DNA polymerase activity with single-nucleotide resolution. *J. Am. Chem. Soc.* **130**, 818–820 (2008).
20. Lieberman, K. R. *et al.* Processive replication of single DNA molecules in a nanopore catalyzed by phi29 DNA polymerase. *J. Am. Chem. Soc.* **132**, 17961–17972 (2010).
- Proof-of-principle experiments demonstrating that a biological nanopore with a coupled polymerase can be used for both strand sequencing and mechanistic studies of enzyme function.**
21. Olasagasti, F. *et al.* Replication of individual DNA molecules under electronic control using a protein nanopore. *Nature Nanotech.* **5**, 798–806 (2010).
22. Rincon-Restrepo, M., Mikhailova, E., Bayley, H. & Maglia, G. Controlled translocation of individual DNA molecules through protein nanopores with engineered molecular brakes. *Nano Lett.* **11**, 746–750 (2011).
23. Mitchell, N. & Howorka, S. Chemical tags facilitate the sensing of individual DNA strands with nanopores. *Angew. Chem. Int. Ed.* **47**, 5565–5568 (2008).
24. Clarke, J. *et al.* Continuous base identification for single-molecule nanopore DNA sequencing. *Nature Nanotech.* **4**, 265–270 (2009).
- Proof-of-principle experiments demonstrating the discrimination of individual mononucleotides using a biological nanopore. Future efforts to couple this with an exonuclease might enable a 'sequencing by digestion' approach.**
25. Stoddart, D., Heron, A. J., Mikhailova, E., Maglia, G. & Bayley, H. Single-nucleotide discrimination in immobilized DNA oligonucleotides with a biological nanopore. *Proc. Natl Acad. Sci. USA* **106**, 7702–7707 (2009).
26. Faller, M., Niederweis, M. & Schulz, G. E. The structure of a mycobacterial outer-membrane channel. *Science* **303**, 1189–1192 (2004).
27. Derrington, I. M. *et al.* Nanopore DNA sequencing with MspA. *Proc. Natl Acad. Sci. USA* **107**, 16060–16065 (2010).
- Proof-of-principle experiments demonstrating duplex interrupted sequencing using MspA are reported here.**
28. Wendell, D. *et al.* Translocation of double-stranded DNA through membrane-adapted phi29 motor protein nanopores. *Nature Nanotech.* **4**, 765–772 (2009).
29. Jing, P., Haque, F., Shu, D., Montemagno, C. & Guo, P. X. One-way traffic of a viral motor channel for double-stranded DNA translocation. *Nano Lett.* **10**, 3620–3627 (2010).
30. Groves, J. T., Ulman, N. & Boxer, S. G. Micropatterning fluid lipid bilayers on solid supports. *Science* **275**, 651–653 (1997).
31. Mager, M. D. & Melosh, N. A. Nanopore-spanning lipid bilayers for controlled chemical release. *Adv. Mater.* **20**, 4423–4427 (2008).
32. White, R. J. *et al.* Ionic conductivity of the aqueous layer separating a lipid bilayer membrane and a glass support. *Langmuir* **22**, 10777–10783 (2006).
33. Venkatesan, B. M. *et al.* Lipid bilayer coated Al₂O₃ nanopore sensors: towards a hybrid biological solid-state nanopore. *Biomed. Microdevices* **13**, 671–682 (2011).
34. Chung, M. & Boxer, S. G. Stability of DNA-tethered lipid membranes with mobile tethers. *Langmuir* **27**, 5492–5497 (2011).
35. Langford, K. W., Penkov, B., Derrington, I. M. & Gundlach, J. H. Unsupported planar lipid membranes formed from mycolic acids of *Mycobacterium tuberculosis*. *J. Lipid Res.* **52**, 272–277 (2011).
36. Knoll, W., Köper, I., Naumann, R. & Sinner, E.-K. Tethered bimolecular lipid membranes — a novel model membrane platform. *Electrochim. Acta* **53**, 6680–6689 (2008).
37. Storm, A. J., Chen, J. H., Ling, X. S., Zandbergen, H. W. & Dekker, C. Fabrication of solid-state nanopores with single nanometre precision. *Nature Mater.* **2**, 537–540 (2003).
38. Venkatesan, B. M. *et al.* Highly sensitive, mechanically stable nanopore sensors for DNA analysis. *Adv. Mater.* **21**, 2771–2776 (2009).
39. Kim, M. J., Wanunu, M., Bell, D. C. & Meller, A. Rapid fabrication of uniformly sized nanopores and nanopore arrays for parallel DNA analysis. *Adv. Mater.* **18**, 3149–3153 (2006).
40. Nam, S.-W., Rooks, M. J., Kim, K.-B. & Rossmagel, S. M. Ionic field effect transistors with sub-10 nm multiple nanopores. *Nano Lett.* **9**, 2044–2048 (2009).
41. McNally, B. *et al.* Optical recognition of converted DNA nucleotides for single-molecule DNA sequencing using nanopore arrays. *Nano Lett.* **10**, 2237–2244 (2010).
- The use of hybridized fluorescent probes allows optical sequence readout.**
42. Li, J. *et al.* Ion-beam sculpting at nanometre length scales. *Nature* **412**, 166–169 (2001).
43. Salisbury, I. G., Timsit, R. S., Berger, S. D. & Humphreys, C. J. Nanometre scale electron beam lithography in inorganic materials. *Appl. Phys. Lett.* **45**, 1289–1291 (1984).
44. Healy, K., Schiedt, B. & Morrison, A. P. Solid-state nanopore technologies for nanopore-based DNA analysis. *Nanomedicine* **2**, 875–897 (2007).
45. Venkatesan, B. M., Shah, A. B., Zuo, J. M. & Bashir, R. DNA sensing using nanocrystalline surface-enhanced Al₂O₃ nanopore sensors. *Adv. Funct. Mater.* **20**, 1266–1275 (2010).
46. Hoogerheide, D. P., Garaj, S. & Golovchenko, J. A. Probing surface charge fluctuations with solid-state nanopores. *Phys. Rev. Lett.* **102**, 256804 (2009).
47. George, S. M. Atomic layer deposition: an overview. *Chem. Rev.* **110**, 111–131 (2009).
48. Geim, A. K. Graphene: status and prospects. *Science* **324**, 1530–1534 (2009).
49. Fischbein, M. D. & Drndic, M. Electron beam nanosculpting of suspended graphene sheets. *Appl. Phys. Lett.* **93**, 113107–113103 (2008).
- This is the first report of nanopore fabrication in a suspended graphene membrane using an electron beam and has led to subsequent studies of DNA translocation through graphene nanopores.**
50. Girit, Ç. Ö. *et al.* Graphene at the edge: stability and dynamics. *Science* **323**, 1705–1708 (2009).
51. Garaj, S. *et al.* Graphene as a subnanometre trans-electrode membrane. *Nature* **467**, 190–193 (2010).
- In addition to containing experimental data showing DNA translocation through a graphene nanopore (see also refs 52 and 53), this paper includes a calculation of the spatial resolution that is possible with monolayer graphene nanopore sensors.**
52. Merchant, C. A. *et al.* DNA translocation through graphene nanopores. *Nano Lett.* **10**, 2915–2921 (2010).
53. Schneider, G. F. *et al.* DNA translocation through graphene nanopores. *Nano Lett.* **10**, 3163–3167 (2010).
54. Hall, J. E. Access resistance of a small circular pore. *J. Gen. Physiol.* **66**, 531–532 (1975).
55. Song, B. *et al.* Atomic-scale electron-beam sculpting of near-defect-free graphene nanostructures. *Nano Lett.* **11**, 2247–2250 (2011).
56. Li, J., Gershow, M., Stein, D., Brandin, E. & Golovchenko, J. A. DNA molecules and configurations in a solid-state nanopore microscope. *Nature Mater.* **2**, 611–615 (2003).
57. Storm, A. J. *et al.* Fast DNA translocation through a solid-state nanopore. *Nano Lett.* **5**, 1193–1197 (2005).
58. Wanunu, M., Morrison, W., Rabin, Y., Grosberg, A. Y. & Meller, A. Electrostatic focusing of unlabelled DNA into nanoscale pores using a salt gradient. *Nature Nanotech.* **5**, 160–165 (2010).
59. Calin, G. A. & Croce, C. M. MicroRNA signatures in human cancers. *Nature Rev. Cancer* **6**, 857–866 (2006).
60. Volinia, S. *et al.* A microRNA expression signature of human solid tumors defines cancer gene targets. *Proc. Natl Acad. Sci. USA* **103**, 2257–2261 (2006).
61. Wanunu, M. *et al.* Rapid electronic detection of probe-specific microRNAs using thin nanopore sensors. *Nature Nanotech.* **5**, 807–814 (2010).
62. Strathdee, G. & Brown, R. Aberrant DNA methylation in cancer: potential clinical interventions. *Expert Rev. Mol. Med.* **4**, 1–17 (2002).
63. Lee, W. H., Isaacs, W. B., Bova, G. S. & Nelson, W. G. CG island methylation changes near the GSTP1 gene in prostatic carcinoma cells detected using the polymerase chain reaction: A new prostate cancer biomarker. *Cancer Epidemiol. Biomarkers* **6**, 443–450 (1997).
64. Laird, P. W. The power and the promise of DNA methylation markers. *Nature Rev. Cancer* **3**, 253–266 (2003).
65. Mirsaidov, U. *et al.* Nanoelectromechanics of methylated DNA in a synthetic nanopore. *Biophys. J.* **96**, L32–L34 (2009).
66. Wanunu, M. *et al.* Discrimination of methylcytosine from hydroxymethylcytosine in DNA molecules. *J. Am. Chem. Soc.* **133**, 486–492 (2010).
67. Botstein, D. & Risch, N. Discovering genotypes underlying human phenotypes: past successes for mendelian disease, future approaches for complex disease. *Nature Genet.* **33**, 228–237 (2003).
68. Zhao, Q. *et al.* Detecting SNPs using a synthetic nanopore. *Nano Lett.* **7**, 1680–1685 (2007).
69. Singer, A. *et al.* Nanopore based sequence specific detection of duplex DNA for genomic profiling. *Nano Lett.* **10**, 738–742 (2010).
70. Iqbal, S. M., Akin, D. & Bashir, R. Solid-state nanopore channels with DNA selectivity. *Nature Nanotech.* **2**, 243–248 (2007).
71. Wanunu, M. & Meller, A. Chemically modified solid-state nanopores. *Nano Lett.* **7**, 1580–1585 (2007).
72. Siwy, Z. S. & Howorka, S. Engineered voltage-responsive nanopores. *Chem. Soc. Rev.* **39**, 1115–1132 (2009).
73. Kowalczyk, S. W. *et al.* Single-molecule transport across an individual biomimetic nuclear pore complex. *Nature Nanotech.* **6**, 433–438 (2011).
74. Yusko, E. C. *et al.* Controlling protein translocation through nanopores with bio-inspired fluid walls. *Nature Nanotech.* **6**, 253–260 (2011).
75. Hall, A. R. *et al.* Hybrid pore formation by directed insertion of alpha-haemolysin into solid-state nanopores. *Nature Nanotech.* **5**, 874–877 (2010).
76. Vercoutere, W. *et al.* Rapid discrimination among individual DNA hairpin molecules at single-nucleotide resolution using an ion channel. *Nature Biotechnol.* **19**, 248–252 (2001).

77. Eid, J. *et al.* Real-time DNA sequencing from single polymerase molecules. *Science* **323**, 133–138 (2009).
78. Drmanac, R. *et al.* Human genome sequencing using unchained base reads on self-assembling DNA nanoarrays. *Science* **327**, 78–81 (2010).
79. Rothberg, J. M. *et al.* An integrated semiconductor device enabling non-optical genome sequencing. *Nature* **475**, 348–352 (2011).
80. <http://www.genome.gov/27527584>.
81. Karnik, R., Duan, C., Castelino, K., Dajugui, H. & Majumdar, A. Rectification of ionic current in a nanofluidic diode. *Nano Lett.* **7**, 547–551 (2007).
82. Jin, X. & Aluru, N. R. Gated transport in nanofluidic devices. *Microfluid. Nanofluid.* **11**, 297–306 (2011).
83. Liu, H. *et al.* Translocation of single-stranded DNA through single-walled carbon nanotubes. *Science* **327**, 64–67 (2010).
84. Nelson, T., Zhang, B. & Prezhdo, O. V. Detection of nucleic acids with graphene nanopores: *ab initio* characterization of a novel sequencing device. *Nano Lett.* **10**, 3237–3242 (2010).
85. Min, S. K., Kim, W. Y., Cho, Y. & Kim, K. S. Fast DNA sequencing with a graphene-based nanochannel device. *Nature Nanotech.* **6**, 162–165 (2011).
86. Postma, H. W. C. Rapid sequencing of individual DNA molecules in graphene nanogaps. *Nano Lett.* **10**, 420–425 (2010).
87. Prasongit, J., Grigoriev, A., Pathak, B., Ahuja, R. & Scheicher, R. H. Transverse conductance of DNA nucleotides in a graphene nanogap from first principles. *Nano Lett.* **11**, 1941–1945 (2011).
88. Luan, B. *et al.* Base-by-base ratcheting of single stranded DNA through a solid-state nanopore. *Phys. Rev. Lett.* **104**, 238103 (2010).
- IBM's DNA transistor architecture and proposed approach to nanopore-based single-molecule DNA sequencing are presented here.**
89. Huang, S. *et al.* Identifying single bases in a DNA oligomer with electron tunnelling. *Nature Nanotech.* **5**, 868–873 (2010).
90. Zwolak, M. & Di Ventra, M. Physical approaches to DNA sequencing and detection. *Rev. Mod. Phys.* **80**, 141–165 (2008).
91. Tanaka, H. & Kawai, T. Partial sequencing of a single DNA molecule with a scanning tunnelling microscope. *Nature Nanotech.* **4**, 518–522 (2009).
92. Tsutsui, M., Taniguchi, M., Yokota, K. & Kawai, T. Identifying single nucleotides by tunnelling current. *Nature Nanotech.* **5**, 286–290 (2010).
- This is the first report of a nanofabricated gap junction being used to discriminate individual nucleotides through electron tunnelling measurements.**
93. Taniguchi, M., Tsutsui, M., Yokota, K. & Kawai, T. Fabrication of the gating nanopore device. *Appl. Phys. Lett.* **95**, 123701–123703 (2009).
94. Ivanov, A. P. *et al.* DNA tunneling detector embedded in a nanopore. *Nano Lett.* **11**, 279–285 (2010).
95. Asmann, Y. W., Kosari, F., Wang, K., Cheville, J. C. & Vasmatzis, G. Identification of differentially expressed genes in normal and malignant prostate by electronic profiling of expressed sequence tags. *Cancer Res.* **62**, 3308–3314 (2002).
96. Feldman, A. L. *et al.* Discovery of recurrent t(6;7)(p25.3;q32.3) translocations in ALK-negative anaplastic large cell lymphomas by massively parallel genomic sequencing. *Blood* **117**, 915–919 (2010).
97. Ling, X. S., Bready, B. & Pertsinidis, A. Hybridization-assisted nanopore sequencing of nucleic acids. US patent 2007 0190542 (2007).
- This approach, called HANS, is being commercially developed by NABsys: 6-mer oligonucleotide probes are hybridized to ssDNA and current versus time traces reveal the position of the probe on the ssDNA template.**
98. Astier, Y., Braha, O. & Bayley, H. Toward single molecule DNA sequencing: direct identification of ribonucleoside and deoxyribonucleoside 5'-monophosphates by using an engineered protein nanopore equipped with a molecular adapter. *J. Am. Chem. Soc.* **128**, 1705–1710 (2006).
99. Lagerqvist, J., Zwolak, M. & Di Ventra, M. Fast DNA sequencing via transverse electronic transport. *Nano Lett.* **6**, 779–782 (2006).
100. Heng, J. B. *et al.* Beyond the gene chip. *Bell Labs Tech. J.* **10**, 5–22 (2005).
101. Gracheva, M. E. *et al.* Simulation of the electric response of DNA translocation through a semiconductor nanopore-capacitor. *Nanotechnology* **17**, 622–633 (2006).
102. Sigalov, G., Comer, J., Timp, G. & Aksimentiev, A. Detection of DNA sequences using an alternating electric field in a nanopore capacitor. *Nano Lett.* **8**, 56–63 (2007).
103. Meller, A., Nivon, L., Brandin, E., Golovchenko, J. & Branton, D. Rapid nanopore discrimination between single polynucleotide molecules. *Proc. Natl Acad. Sci. USA* **97**, 1079–1084 (2000).
104. Howorka, S., Cheley, S. & Bayley, H. Sequence-specific detection of individual DNA strands using engineered nanopores. *Nature Biotechnol.* **19**, 636–639 (2001).
105. Bates, M., Burns, M. & Meller, A. Dynamics of DNA molecules in a membrane channel probed by active control techniques. *Biophys. J.* **84**, 2366–2372 (2003).
106. Borsenberger, V., Mitchell, N. & Howorka, S. Chemically labeled nucleotides and oligonucleotides encode DNA for sensing with nanopores. *J. Am. Chem. Soc.* **131**, 7530–7531 (2009).
107. Chen, P. *et al.* Probing single DNA molecule transport using fabricated nanopores. *Nano Lett.* **4**, 2293–2298 (2004).
108. Storm, A. J., Chen, J. H., Zandbergen, H. W. & Dekker, C. Translocation of double-strand DNA through a silicon oxide nanopore. *Phys. Rev. E* **71**, 051903 (2005).
109. Fologea, D., Uplinger, J., Thomas, B., McNabb, D. S. & Li, J. Slowing DNA translocation in a solid-state nanopore. *Nano Lett.* **5**, 1734–1737 (2005).
110. Kim, Y. R. *et al.* Nanopore sensor for fast label-free detection of short double-stranded DNAs. *Biosensors Bioelectron.* **22**, 2926–2931 (2007).
111. Wanunu, M., Sutin, J., McNally, B., Chow, A. & Meller, A. DNA translocation governed by interactions with solid-state nanopores. *Biophys. J.* **95**, 4716–4725 (2008).
112. Chen, Z. *et al.* DNA translocation through an array of kinked nanopores. *Nature Mater.* **9**, 667–675 (2010).

Acknowledgements

B.M.V. is a trainee supported by the Midwestern Cancer Nanotechnology Training Center (NIH-NCI R25 CA154015). Support from the National Institutes of Health (R21 CA155863) and the National Science Foundation (EEC-0425626) is also acknowledged. The authors thank J. Hanlon-Sinn (Beckman Institute of Advanced Technology, University of Illinois at Urbana-Champaign) for the images in Fig. 6, and M. Drndic (University of Pennsylvania) for valuable discussions.

Additional information

The authors declare no competing financial interests.